Bufotalin induces cell cycle arrest and cell apoptosis in human malignant melanoma A375 cells

ZHAOHAI PAN[1], CHUANJUN QU[1], YING CHEN[1], XIAOYU CHEN[1], XIAONA LIU[1], WENJIN HAO[1], WENJUAN XU[1], LEI YE[1], PENG LU[3], DEFANG LI[1] and QIUSHENG ZHENG[1,2]

[1]School of Integrated Traditional Chinese and Western Medicine, Binzhou Medical University, Yantai, Shandong 264003; [2]Key Laboratory of Xinjiang Endemic Phytomedicine Resources of Ministry of Education, School of Pharmacy, Shihezi University, Shihezi, Xinjiang 832002; [3]Department of Education, Yantai Affiliated Hospital of Binzhou Medical University, Yantai, Shandong 264003, P.R. China

Received July 18, 2018; Accepted February 22, 2019

DOI: 10.3892/or.2019.7032

Abstract. Venenum bufonis has been used as an antitumor drug in China for many years. Bufotalin, as an active component of Venenum bufonis, has been proven to exhibit antitumor effects in cancer types. In the present study, the effect of bufotalin on the human melanoma skin cancer cell line A375 was analyzed using MTT and colony formation assays. Bufotalin significantly inhibited the proliferation and colony formation of A375 cells. Further studies demonstrated that bufotalin significantly upregulated the protein levels of ATM serine/threonine kinase and Chk2, downregulated CDC25C protein expression, and subsequently inhibited CDK1 expression, leading to cell cycle arrest at the G2/M phase of the A375 cells. Furthermore, bufotalin significantly increased BAX expression levels, decreased BCL-2 expression, and then upregulated apoptosis-related proteins, caspase-3/-9, followed by A375 cell apoptosis. Taken together, these results show that bufotalin induces cell cycle arrest at the G2/M phase and cell apoptosis, resulting in the inhibition of A375 cell proliferation, thereby suggesting that bufotalin may be utilized in melanoma treatment.

Introduction

Cutaneous malignant melanoma (CMM) is a highly malignant and invasive skin tumor that has a high incidence rate in Japan, Europe and other countries (1). CMM occurs in the surface of the skin or in mucous membranes, including the leptomeninges and the choroid (2). According to the origin and site of melanoma, CMM includes four pathological types, namely, superficial spreading type melanoma, acral lentiginous melanoma, nodular melanoma and lentigo malignant melanoma (3). Clinical data demonstrate that melanoma is the fifth most common cancer in males and fifth most common cancer in females in the US (4). Even though the incidence rates are lower in Asian countries, the incidence rate of melanoma has reached to 1/100,000 in China (5).

The occurrence of malignant melanoma is a complex process with multiple factors and steps (6). A previous study has reported that the cause of malignant melanoma includes sun exposure, ultraviolet light (UV) exposure, ionizing radiation and genetic factors (7). UV rays can penetrate the skin's surface and cause the destruction of collagen and elastic proteins in the skin, leading to malignant melanoma. Furthermore, sex, age, skin color and race are factors that are associated with incidence of malignant melanoma (8). For Caucasians, superficial diffuse melanoma is the most frequent melanoma and accounts for ~90% of all malignant melanoma cases. For persons of Asian and African descent, freckle-like melanoma accounts for 50-70% of all patients with malignant melanoma (9,10). In addition, malignant melanoma may be inherited, and it has been suggested that 10% of patients with melanoma have a family history (11).

To date, vemurafenib, ipilimumab, sibutramine and other targeted drugs have been recommended for the treatment of malignant melanoma. However, malignant melanoma is not completely cured by these agents (12). Metastasis may occur during the early stages of cutaneous malignant melanoma and prognosis is often poor. Metastasis is also an important cause of high mortality. In addition, multidrug resistance has been reported in the chemotherapy of melanoma, leading to a very poor prognosis (13); thus, there is a need to identify novel therapeutic drugs and drug targets for melanoma.

Bufotalin, a compound of the traditional Chinese medicine Venenum bufonis, is isolated from the dried secretions of the auricular and skin glands of *Bufo gargarizans* Cantor (14). Venenum bufonis has been used to treat various conditions, including cardiac illness, pain and cancer, in China and other

Correspondence to: Professor Defang Li or Professor Qiusheng Zheng, School of Integrated Traditional Chinese and Western Medicine, Binzhou Medical University, 346 Guanhai Road, Yantai, Shandong 264003, P.R. China
E-mail: lidefang@163.com
E-mail: zqsyt@sohu.com

Key words: bufotalin, melanoma, A375 cells, apoptosis, cell cycle arrest

Asian countries. Venenum bufonis has been historically used as an oral or topical anti-neoplastic drug in China (15). A previous study has shown that bufotalin is a bufadienolide, a C-24 steroidal compound, and one of the main active components of Venenum bufonis (16). *In vitro* investigations have demonstrated that bufotalin can effectively inhibit the proliferation of hepatoma cells, gastric cancer cells, and sarcoma cells (17). Bufotalin also inhibits the growth of liver cancer and sarcoma in animal models of transplanted tumors, and without obvious side-effects; however, the antitumor effect of bufotalin on malignant melanoma has not been investigated to date.

The present study examined the *in vitro* effects of bufotalin on human malignant melanoma A375 cells and explored its underlying molecular mechanism. We found that bufotalin remarkably induced cell cycle arrest at the G2/M phase and cell apoptosis, which in turn inhibited cellular proliferation. These findings suggest that bufotalin may be a potential chemotherapeutic agent for malignant melanoma treatment.

Materials and methods

Cell culture. Human malignant melanoma A375 cells (cat. no. SCSP-533) were purchased from Cell Bank, Typical Culture Preservation Commission, Chinese Academy of Sciences (Shanghai, China). The normal human keratinocyte cell line HaCaT (cat. no. CL-0090; STR profiling authentication) was purchased from Procell Life Science & Technology Co., Ltd. (Wuhan, China). The cells were cultured with Dulbecco's modified Eagles' medium (DMEM)/high-glucose basal medium (HyClone; GE Healthcare Life Sciences, Logan, UT, USA), containing 10% fetal calf serum (Gibco; Thermo Fisher Scientific, Inc., Waltham, MA, USA), 1% sodium pyruvate (Beijing Solarbio Science & Technology Co., Ltd., Beijing, China), 0.1 U/l penicillin, and 0.1 μg/l streptomycin (Beijing Solarbio Science & Technology Co., Ltd.) and incubated in a 5% CO_2 incubator at 37˚C. Fetal calf serum was inactivated in a 56˚C water bath for 30 min before use.

MTT assay. The effect of bufotalin on the viability of A375 and HaCaT cells was determined by an MTT assay. The cells in suspension ($1x10^4$ cells in 100 μl DMEM) were seeded into 96-well plates. After 24 h of incubation, different concentrations of bufotalin (cat. no. ASB-00002466-005; J&K Scientific Ltd., Beijing, China) were added, and the cells were further cultured for 24 and 48 h. Then, 10 μl MTT solution (5 mg/ml) was added into each well, and the cells were incubated for an additional 2 h. The resulting formazan crystals were dissolved using 150 μl dimethyl sulfoxide (DMSO). Absorbance was measured at a wavelength of 490 nm using a microplate reader (Bio-Rad Laboratories, Inc., Hercules, CA, USA). The absorbance of the cells treated with DMEM medium containing 0.1% DMSO was regarded as the control group (survival rate 100%). IC_{50} represents the drug concentration causing a 50% decrease in survival rate.

Colony formation assay. The A375 cells were trypsinized, collected, and diluted into 300 cells in 1 ml DMEM medium. The cell suspension was seeded into a 6-well plate at 300 cells/well. After culturing for 24 h, the cells were treated with different concentrations of bufotalin for 24 h. Then, the treated cells were incubated with DMEM complete medium at 37˚C for 14 days. Finally, cells were fixed in 4% paraformaldehyde solution for 15 min at room temperature, and the cells were stained with Giemsa solution at room temperature for 10 min, then examined and images under a light microscope. The colonies containing >50 cells were counted and used to calculate the colony formation rate.

Hoechst 33258 staining. The A375 cells ($6x10^5$ cells) were seeded onto sterile cover slips and placed into 6-well plates and cultured for 24 h. Then, the cells were treated with different concentrations of bufotalin. After 12 h of treatment, the cells were fixed in 4% paraformaldehyde solution for 15 min at room temperature, washed twice with PBS, and then the cells were stained with Hoechst 33258 (cat. no. C1018; Beyotime Institute of Biotechnology, Haimen, China) at room temperature for 10 min. Stained nuclei were observed, and images were captured using a fluorescence microscope. Apoptotic cells (cells exhibiting nuclear fragmentation and/or with distinct apoptotic bodies) were counted, and the percentage of apoptotic cells (number of apoptotic cells/the total number of cells x 100) was calculated.

Cell cycle analysis. Cell cycle distribution of the bufotalin-treated A375 cells was assessed by flow cytometry. Briefly, the bufotalin-treated A375 cells (~$8x10^5$ cells/group) were collected and fixed in 70% ethanol at 4˚C overnight. After fixation, the cells were centrifuged at 800 x g for 5 min to remove the ethanol. Then, the cells were suspended in 500 μl PBS containing 0.02 mg/ml propidium iodide (PI) and 0.1 mg/ml ribonuclease A (RNase A) in darkness at 37˚C for 30 min. The fluorescence emitted by the PI-DNA complexes was measured using an Epics XL flow cytometry (Beckman Coulter, Inc., Brea, CA, USA). Cell distribution in different phases of the cell cycle was analyzed using WinMDI 2.8 software (The Scripps Research Institute, La Jolla, CA, USA).

Annexin V-fluorescein isothiocyanate (FITC)/PI double staining assay. Annexin V-FITC/PI double staining assay (Annexin V-FITC Apoptosis Detection Kit; cat. no. CA1020; Beijing Solarbio Science & Technology Co., Ltd.) was performed according to the manufacturer's instructions. Briefly, A375 cells (~$8x10^5$ cells/group) were harvested at 24 h after bufotalin treatment and then incubated in 100 μl labeling solution, which consisted of 5 μl Annexin V-FITC, 10 μl PI, 10 μl 10X binding buffer and 75 μl H_2O in darkness at room temperature for 15 min. Then, 400 μl 1X binding buffer were added to stop the staining reaction. The stained cells were detected using FL1 and FL3 fluorescence channels on a FACSort flow cytometry system (FACSCanto II; Becton, Dickinson and Company, Franklin Lakes, NJ, USA), and the percentages of apoptotic cells in each group were analyzed using BD FACSDiva software (version 6.1.3; BD Biosciences, Becton, Dickinson and Company).

Western blot analysis. A375 cells ($1x10^6$/well) were seeded in 100-mm culture dishes and treated with different concentrations of bufotalin for 24 h. Following treatment, cells were collected and incubated in cell lysis buffer (20 mM Tris-HCl, 150 mM NaCl, 1 mM EDTA, 1% Triton X-100, 2.5 mM sodium

pyrophosphate, 0.1 mM phenylmethanesulfonylfluoride, 0.1 mM sodium orthovanadate, 0.5 mM dithiothreitol and 10X protease inhibitor; pH 6.8) on ice for 30 min. Cells were vortexed for 45 sec and then centrifuged at 10,000 x g at 4˚C for 10 min. The supernatant was collected and stored at -20˚C. Protein concentrations were determined using a bicinchoninic acid protein assay kit (Beijing Solarbio Science & Technology Co., Ltd.). Cell lysates with a protein content of 40 mg were mixed with an equal volume of sodium dodecyl sulfate (SDS) loading dye (2% SDS, 10% sucrose, 0.002% bromophenol blue, 5% 2-mercaptoethanol and 625 mM Tris; pH 6.8) and subsequently separated by SDS-PAGE on 12.5% gels along with a rainbow-colored protein molecular marker (Beijing Solarbio Science & Technology Co., Ltd.). After running for 2 h at 110V, the proteins were transferred to polyvinylidene fluoride membranes (EMD Millipore, Billerica, MA, USA) using a Trans-blots SD semi-dry transfer cell (Bio-Rad Laboratories, Inc.). The membranes were blocked with 5% bovine serum albumin (BSA; cat. no. A8010; Beijing Solarbio Science & Technology Co., Ltd.) in Tris-buffered saline containing 0.1% Tween-20 (TBS-T) for 60 min before being probed with primary antibodies [protein kinase B (AKT), cat. no. ab38449, 1:500; phosphorylated (p)-AKT, cat. no. ab38449, 1:500; ATM serine/threonine kinase (ATM), cat. no. ab78, 1:1,000; checkpoint kinase 2 (Chk2), cat. no. ab47433, 1:1,000; cell division cycle 25C (CDC25C), cat. no. ab32444, 1:1,000; cyclin-dependent kinase 1 (CDK1), cat. no. ab18, 1:1,000; cyclin B, cat. no. ab181593, 1:1,000; BCL2-associated X, apoptosis regulator (BAX), cat. no. ab32503, 1:1,000; B cell lymphoma-2 (BCL-2), cat. no. ab32124, 1:1,000; caspase-3, cat. no. ab13585, 1:1,000; caspase-9, cat. no. ab202068, 1:1,000; all Abcam, Cambridge, UK] containing 5% BSA at 4˚C overnight. Subsequently, the membranes were washed with TBS-T buffer for 45 min and then probed with appropriate secondary antibodies (goat anti-mouse IgG H&L, cat. no. ab205719, 1:20,000; or goat anti-rabbit IgG H&L, cat. no. ab6721, 1:20,000; Abcam) conjugated with horseradish peroxidase for 1 h at room temperature. Immunoreactive bands were visualized with enhanced chemiluminescence detection reagents (Invitrogen; Thermo Fisher Scientific, Inc.) using a film processor (Kodak, Rochester, NY, USA), and the gray-scale values of each image were analyzed using Image-Pro Plus 6.0 (IPP6) software.

Statistical analysis. The experiments were conducted at least three times. All the data are expressed as the mean ± standard deviation. Analyses were performed using the SPSS 21.0 software package (version 21.0; IBM Corp., Armonk, NY, USA). Student's t-test, a one-way analysis of variance (ANOVA) or a two-way ANOVA was used to calculate statistical differences, respectively. Tukey's post hoc tests were undertaken following a significant one-way ANOVA, and Bonferroni's post hoc tests were undertaken following a significant two-way ANOVA. $P<0.05$ was considered to indicate a statistically significant difference.

Results

In vitro anti-melanoma effects of bufotalin. To examine the antiproliferative effect of bufotalin on human malignant melanoma A375 cells, the cells were treated with or without various concentrations of bufotalin for 24 and 48 h, then the viability of bufotalin-treated cells was determined by the MTT assay. Bufotalin (10-80 ng/ml) significantly inhibited A375 cell proliferation, with an IC_{50} value of 40 ng/ml after 24 h treatment (Fig. 1A). Furthermore, the proliferation rate was significantly lower in A375 cells after 48 h treatment with bufotalin than that in A375 cells after 24 h treatment with the same concentration (10-80 ng/ml) of bufotalin (Fig. 1A). Subsequently, according to the IC_{50} value of bufotalin (40 ng/ml), we selected 30, 40 and 50 ng/ml as the concentrations of bufotalin used in the next studies. Additionally, light microscopy indicated changes in cell number and cell morphology. There was a marked decrease in the number of A375 cells after treatment with bufotalin, and some cells began to shrink and deform, and even detach from the dish surface (Fig. 1B). In addition, bufotalin significantly inhibited A375 cell colony formation at concentrations of 30, 40 and 50 ng/ml (Fig. 1C and D). Bufotalin also effectively inhibited HaCaT cell proliferation at 50-80 ng/ml after 24 h treatment, whereas the cytotoxicity of bufotalin on HaCaT cells is significantly lower than that on A375 cells (Fig. 1E).

Bufotalin induces cell cycle arrest at the G2/M phase in A375 cells. To explore the mechanism of action underlying the bufotalin-mediated antiproliferative effect, the cell cycle distribution profile of bufotalin-treated A375 cells was investigated. After exposure of A375 cells to bufotalin for 24 h, a marked accumulation of cells at the G2/M phase compared with the control group was observed (Fig. 2A and B). The protein levels of G2/M phase regulatory proteins, CDK1 and cyclin B, were subsequently analyzed by western blot analysis. The results demonstrated that the CDK1 protein expression levels in bufotalin-treated A375 cells significantly decreased compared to the control group, whereas no change in cyclin B protein expression levels in bufotalin-treated A375 cells was detected (Fig. 2C and D). These results indicated that bufotalin effectively inhibited the expression of CDK1, but not cyclin B.

Effects of bufotalin on ATM/Chk2/CDC25C signaling. Considering the cell cycle arrest at the G2/M phase and the decreased ratio of CDK1/cyclin B in bufotalin-treated A375 cells, changes in the levels of the components of the ATM/Chk2/CDC25C signaling pathway, which regulates cell transmission through the G2/M phase (18), were examined by western blot analysis. The results demonstrated that the protein levels of ATM and Ckh2 were significantly higher, and that of CDC25C was significantly lower in bufotalin-treated A375 cells compared to the control group (Fig. 3A and B).

Bufotalin promotes cell apoptosis in A375 cells. In the above experiment, bufotalin effectively inhibited A375 cell proliferation through G2/M cell cycle arrest. Additionally, the changes in A375 cell morphology that were induced by bufotalin were similar to those observed during apoptosis. To explore whether this proliferation inhibition is associated with cell apoptosis, the bufotalin-treated A375 cells were stained with Hoechst 33258 and examined by fluorescence microscopy. The typical apoptosis characteristics, nuclear shrinkage, DNA condensation, and apoptotic bodies, were observed in

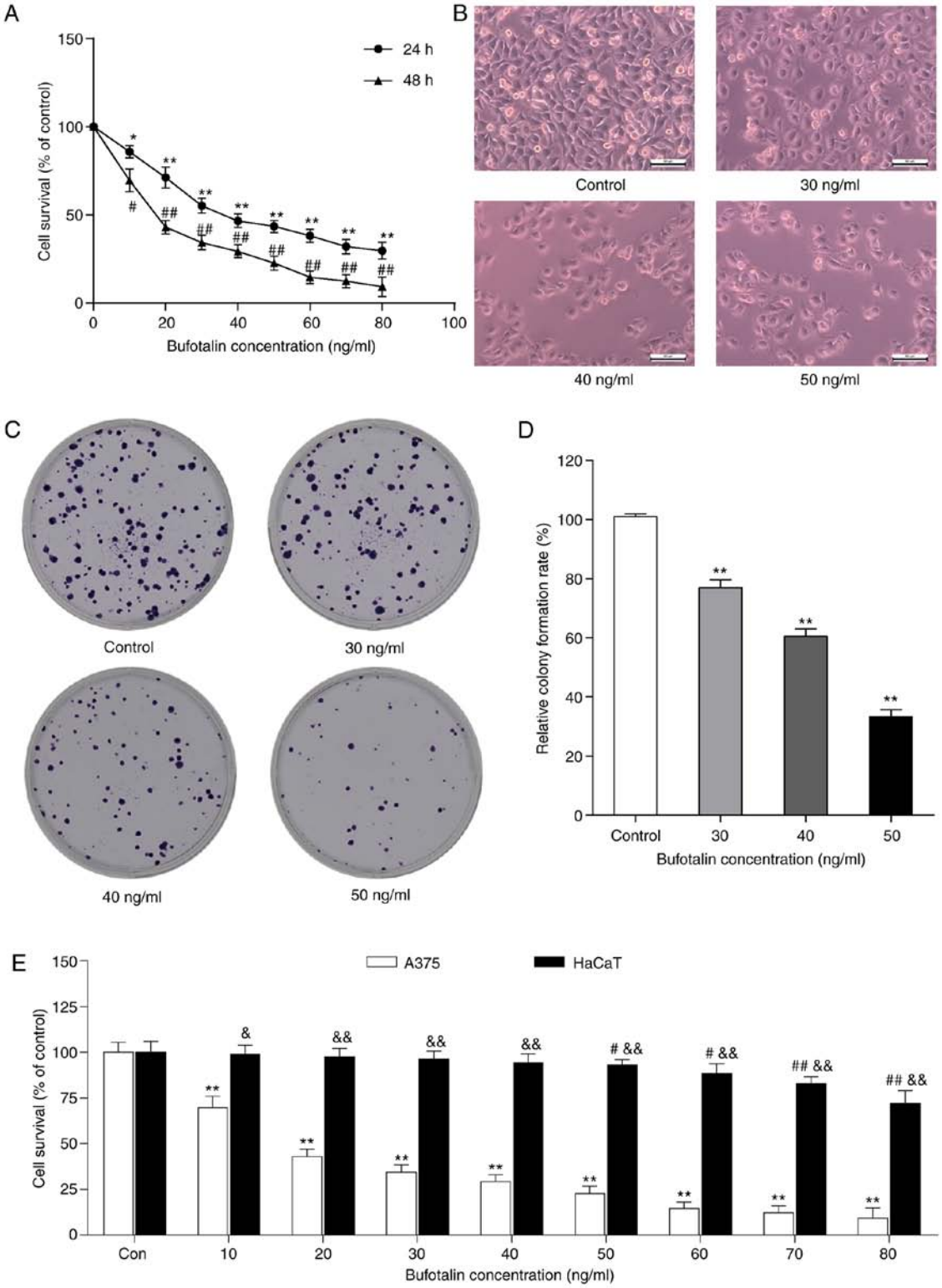

Figure 1. Inhibitory effect of bufotalin on the viability of A375 cells. (A) Cells were seeded into 96-well plates and treated with different concentrations of bufotalin for 24 and 48 h. The viability of bufotalin-treated cells was determined using the MTT assay. *P<0.05, **P<0.01 vs. A375 cells control group (24 h); $^{\#}$P<0.05 vs. A375 cells treated with the different concentrations of bufotalin for 24 or 48 h. (B) Changes in the morphology of bufotalin-treated A375 cells were observed using phase-contrast microscopy. Scale bar, 50 μm. (C) Representative images of A375 cell colony formation following treatment with bufotalin. (D) Data analysis of bufotalin-treated A375 cell colony formation. (E) The viability of A375 cells and HaCaT cells was determined using the MTT assay following the treatment with different concentrations of bufotalin for 24 h. *P<0.05, **P<0.01 vs. A375 cells control group; $^{\#}$P<0.05 vs. HaCaT cells control group. $^{\&}$P<0.05, $^{\&\&}$P<0.01 vs. A375 cells treated with the same concentration of bufotalin. All data are presented as the mean ± standard deviation of three independent experiments.

bufotalin-treated A375 cells (Fig. 4A and B). Furthermore, the apoptotic rate of bufotalin-treated A375 cells was determined using an Annexin V FITC/PI double staining assay and flow cytometry analysis. The percentage of apoptotic cells was

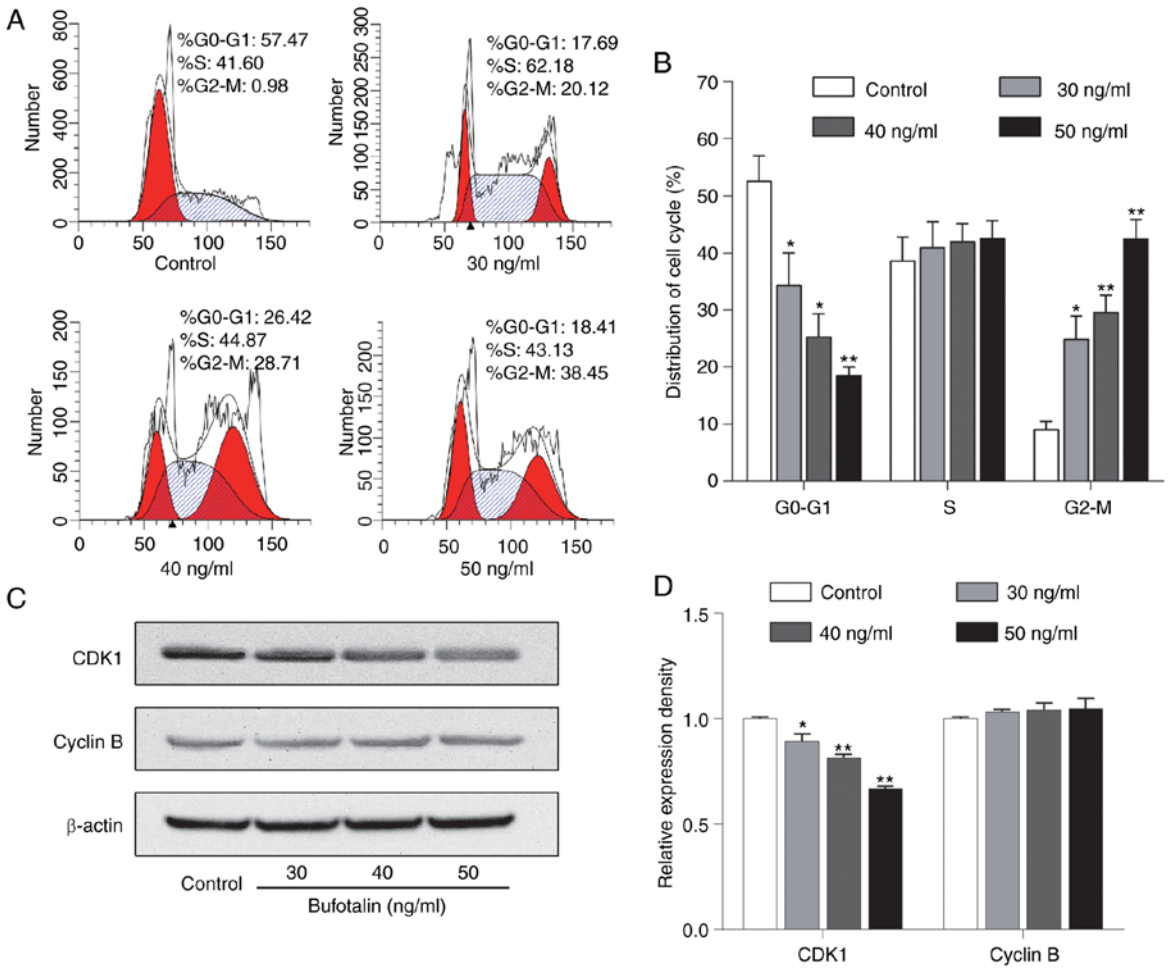

Figure 2. Bufotalin induces cell cycle arrest of A375 cells at the G2/M phase. (A) Representative images of bufotalin-treated A375 cell cycle distribution determind by flow cytometry. (B) Statistical analysis of bufotalin-treated A375 cell cycle distribution. (C) The protein levels of CDK1 and cyclin B in bufotalin-treated A375 cells were detected by western blot analysis. (D) Statistical analysis of the relative protein levels of CDK1 and cyclin B in bufotalin-treated A375 cells. The relative protein ratios were normalized to the values of the control group. All data are presented as the mean ± standard deviation of three independent experiments. *P<0.05, **P<0.01 vs. control group. CDK1, cyclin-dependent kinase 1.

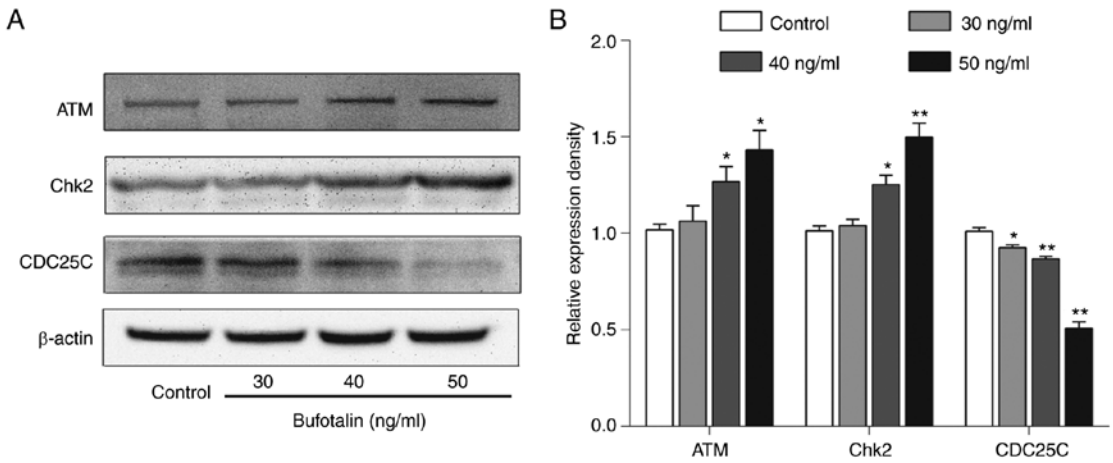

Figure 3. Effects of bufotalin on the protein levels of ATM/Chk2/CDC25C signaling molecules. (A) The protein levels of ATM, Chk2 and CDC25C in bufotalin-treated A375 cells were detected by western blotting. (B) Statistical analysis of the relative protein levels of ATM, Chk2, and CDC25C in bufotalin-treated A375 cells. The relative protein ratios were normalized to the values of the control group. All data are presented as the mean ± standard deviation of three independent experiments. *P<0.05, **P<0.01 vs. control group. ATM, ATM serine/threonine kinase; Chk2, checkpoint kinase 2; CDC25C, cell division cycle 25C.

significantly increased with increasing bufotalin concentration (Fig. 4C and D). These results suggested that bufotalin induced cell apoptosis in A375 cells, leading to an antiproliferative effect.

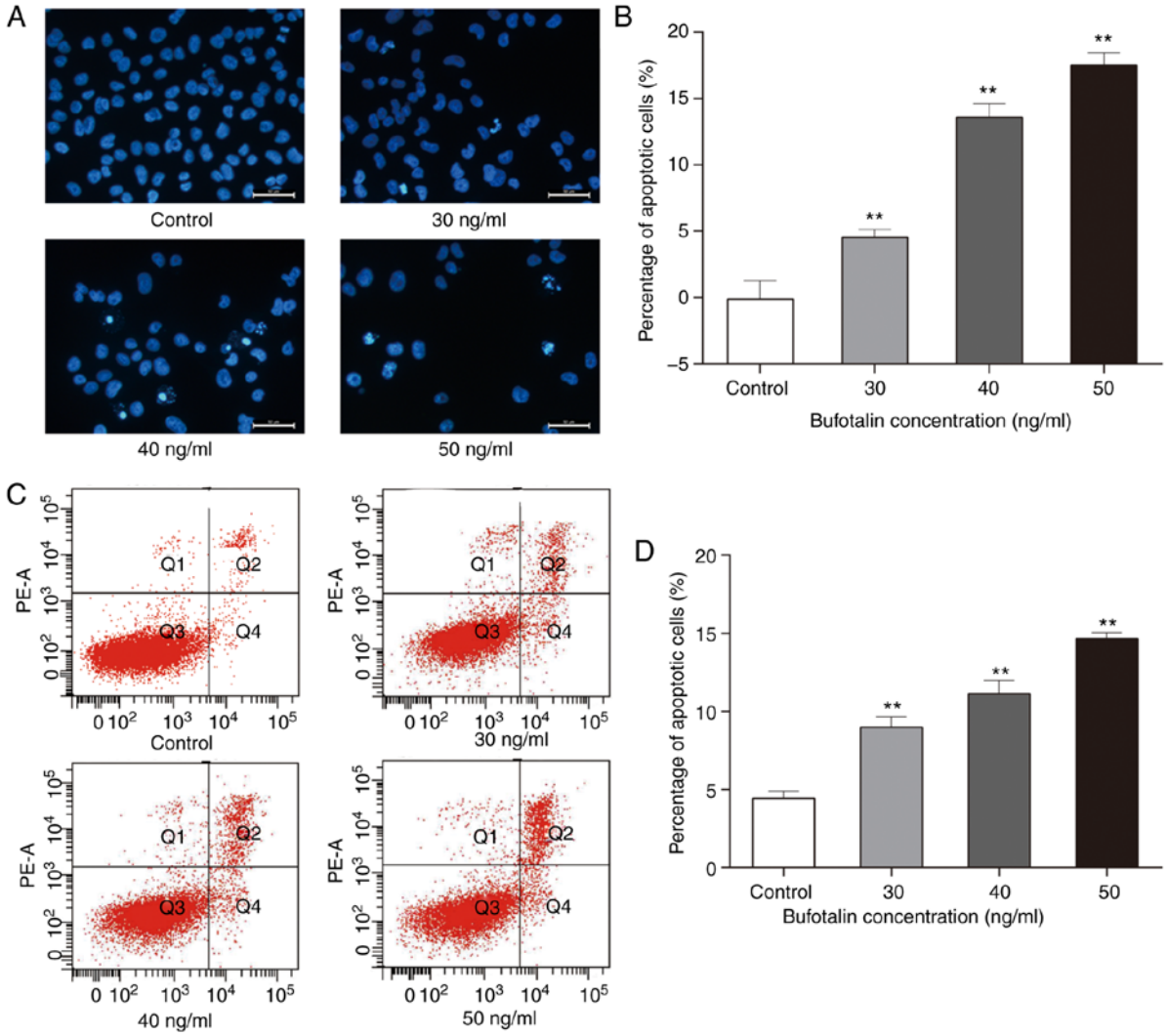

Figure 4. Bufotalin induces cell cycle arest at G2/M phase in A375 cells. (A) Representative images of the morphological changes of bufotalin-treated A375 cells after staining with Hoechst dye 33258. (B) Statistical analysis of the percentage of apoptotic cells in bufotalin-treated A375 cells using Hoechst 33258 staining. (C) The apoptotic rate of bufotalin-treated A375 cells was determined using an Annexin V-fluorescein isothiocyanate/propidium iodide double staining assay. (D) Statistical analysis of the apoptotic rate in bufotalin-treated A375 cells. All data are presented as the mean ± standard deviation of three independent experiments. $^{**}P<0.01$ vs. control group.

Effects of bufotalin on apoptosis-associated signaling pathways. The levels of cell apoptosis-associated proteins, BCL-2, BAX, caspase-3 and -9, were detected in A375 cells by western blot analysis. The level of BCL-2 was significantly downregulated and the levels of BAX, caspase-3 and -9 were markedly upregulated in bufotalin-treated A375 cells compared with the control group (Fig. 5A and B). Additionally, considering the regulatory effect of the activation of AKT on caspase-3/-9, the levels of AKT and p-AKT in bufotalin-treated A375 cells. Bufotalin markedly decreased p-AKT levels and the ratio of p-AKT/AKT, whereas no significant change in AKT expression levels was observed in A375 cells following bufotalin treatment (Fig. 5C and D).

Discussion

It has been reported that bufotalin, a bufadienolide, has strong antitumor efficacy in several tumor cell lines, including gastric cancer, liver cancer, hepatoma and sarcoma cells (17,19). The present study explored the effect of bufotalin on human malignant melanoma A375 cell proliferation and its associated mechanism. Bufotalin effectively suppressed the proliferation of melanoma A375 cells by arresting them at the G2/M phase and inducing cell apoptosis.

The cell cycle, which is a complex cell division process, has an important role in cell proliferation. Cyclins and CDKs are the direct regulatory factors of the cell cycle, which have important roles in normal and tumor cells (20). Cyclin B, in complex with CDK1, triggers mitotic entry and is a key modulator of the G2/M checkpoint (21). It has been reported that coffee oil-algae oil nanoemulsions upregulated the protein level of cyclin B and downregulated the protein level of CDK1, subsequently causing cell cycle arrest of B16-F10 cells at the G2/M phase (22). By contrast, immature colon carcinoma transcript-1 knockdown downregulated the levels of cyclin B and CDK1, arresting human breast cancer ZR-75-30 cells at G2/M phase (23). Thus, it is uncertain whether the level of cyclin B is upregulated/downregulated in G2/M phase-arrested cells. However, several studies showed that the downregulation of CDK1/cyclin B complex/activity is associated with

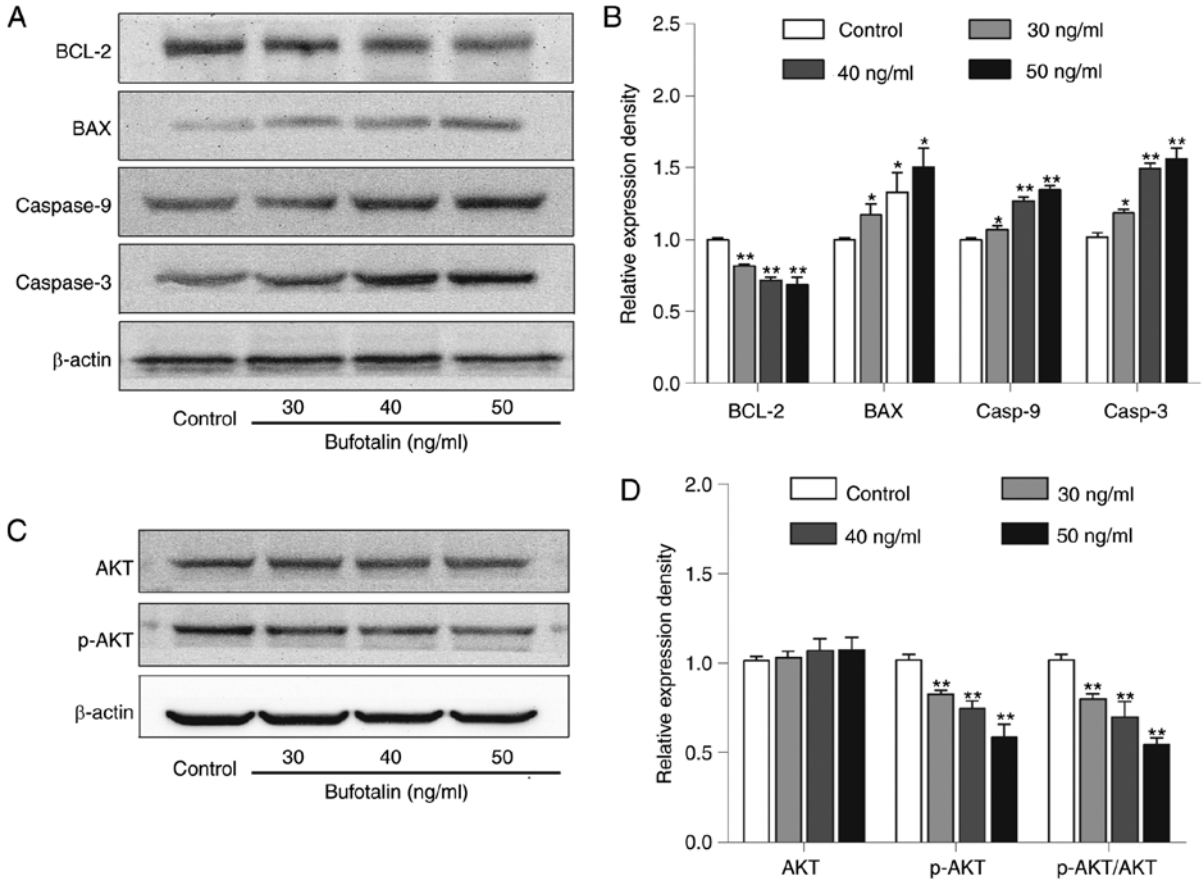

Figure 5. Effects of bufotalin on the protein levels of apoptosis-associated signaling molecules. (A) The protein levels of BAX, BCL-2, caspase-3 and -9 in bufotalin-treated A375 cells were assessed by western blotting. (B) Statistical analysis of the relative protein levels of BAX, BCL-2, caspase-3 and -9 in bufotalin-treated A375 cells. (C) Western blot analysis for the protein levels of AKT and p-AKT in bufotalin-treated A375 cells. (D) Statistical analysis of the relative protein levels of AKT and p-AKT. All data are presented as the mean ± standard deviation of three independent experiments. *P<0.05, **P<0.01 vs. control group. BAX, BCL2-associated X, apoptosis regulator; BCL-2, B cell lymphoma-2; AKT, protein kinase B; p-, phosphorylated.

cell cycle arrest at G2/M phase (24-26). Consistent with these studies, bufotalin decreased the level of CDK1, which could downregulate the level of CDK1/cyclin B complex, leading to cell cycle arrest at G2/M phase in bufotalin-treated A375 cells in the present study.

Several studies have demonstrated that cells with DNA damage do not pass through G2/M phase, resulting in an increase in the number of cells arrested at the G2/M phase (27). Thus, the appearance of G2/M cell cycle arrest in bufotalin-treated A375 cells suggests that the cells may have incurred DNA damage and repair. It has been reported that the signal pathway mediated by the ATM/ATR serine/threonine kinase protein repairs damaged DNA (28). DNA damage caused by various causes can activate ATM (29), which subsequently upregulates Chk2 and downregulates CDC25C, leading to cell cycle arrest at the G2/M phase (30). The present data is consistent with the above studies, wherein bufotalin upregulates ATM in A375 cells, followed by an increase in Chk2 and decrease in CDC25C expression, leading to cell cycle arrest at the G2-M phase.

It has been reported that bufotalin can induce cell apoptosis in HeLa cells and drug-resistant HepG2 cells by regulating the expression of caspase family proteins (17). In the current study, the levels of caspase-3 and -9 were significantly increased in A375 cells after bufotalin treatment for 24 h. Furthermore, changes in mitochondrial apoptosis-associated proteins, BCL-2 and BAX were observed in bufotalin-treated A375 cells, indicating that bufotalin may induce apoptosis via the mitochondrial apoptosis pathway. Additionally, it has been reported that the upregulation of AKT, an anti-apoptotic protein (31), in tumor cells leads to rapid growth of tumor cells, and activated AKT is also an inhibitor of caspase-3 and -9 (32). Bufotalin effectively inhibited the phosphorylation of AKT in A375 cells. This result indicated that bufotalin inhibits AKT phosphorylation and subsequently increases the levels of downstream executioner caspases (caspase-3 and -9), leading to A375 cell apoptosis.

Notably, there are some safety concerns regarding the treatment of melanoma using natural compounds, even when these traditional medicines have been used for thousands of years. The data of the present study demonstrated that bufotalin could inhibit HaCaT cell proliferation at 50-80 ng/ml, but bufotalin significantly inhibited A375 cell proliferation at a lower dose (10 ng/ml). It is suggested that bufotalin has a certain degree of selectivity against malignant melanoma compared with normal skin cells.

Additionally, there are certain limitations to this study. The anti-melanoma effect of bufotalin was only evaluated in one human melanoma cell line, A375, and thus other skin cancer cells (e.g. mouse malignant melanoma B16 cells) will

be using to further explore the therapeutic effect of bufotalin in subsequent studies. Furthermore, the effect of bufotalin in an A375-xenografted model in nude mice has not been determined.

In conclusion, the results demonstrated that bufotalin simultaneously induces cell cycle arrest and apoptosis in A375 cells. Further studies revealed that bufotalin could induce cell cycle arrest at G2/M phase by upregulating ATM and Chk2, and downregulating Cdc25C. Bufotalin also induces cell apoptosis via the mitochondrial apoptosis pathway and inhibition of AKT phosphorylation. The results provide a strong basis for developing bufotalin into a potential therapeutic agent for the treatment of cutaneous malignant melanoma.

Acknowledgements

Not applicable.

Funding

The National Natural Science Foundation of China (grant nos. 81872162 and 81602556 to DL; grant no. 31870338 to QZ), the Natural Science Foundation of Shandong Province (grant no. ZR2017JL030 to DL), Taishan Scholars Construction Engineering of Shandong Province (to DL), Yantai High-End Talent Introduction Plan 'Double Hundred' (to DL), the Scientific Research Foundation of Binzhou Medical University (grant no. BY2016KYQD01 to DL) and the Dominant Disciplines' Talent Team Development Scheme of Higher Education of Shandong Province (to DL) supported this study.

Availability of data and materials

The datasets used during the present study are available from the corresponding author upon reasonable request.

Authors' contributions

ZP, DL and QZ designed the study, acquired the data and wrote the manuscript; CQ, YC, XC and XL collected cell samples for Hoechst 33258 staining, cell cycle and western blot analyses; WH, WX, LY and PL interpreted and analyzed the data; DL and QZ revised and approved the final version of the manuscript. All authors read and approved the manuscript and agree to be accountable for all aspects of the research in ensuring that the accuracy or integrity of any part of the work are appropriately investigated and resolved.

Ethics approval and consent to participate

Not applicable.

Patient consent for publication

Not applicable.

Competing interests

The authors declare that they have no competing interests.

References

1. Saida T: Melanoma and Non-melanoma skin cancers. Gan To Kagaku Ryoho 45: 612-613, 2018 (In Japanese).
2. Gallego Y, Mendicute J, Ruiz M, Ruiz I and Ubeda M: Melanocytoma of the ciliary body. Arch Soc Esp Oftalmol 80: 109-112, 2005 (In Spanish).
3. Lang J and MacKie RM: Prevalence of exon 15 *BRAF* mutations in primary melanoma of the superficial spreading, nodular, acral, and lentigo maligna subtypes. J Invest Dermatol 125: 575-579, 2005.
4. Nakamura Y: II. Diagnosis and treatment for nail Apparatus (Subungual) Melanoma]. Gan to Kagaku Ryoho 45: 619-621, 2018 (In Japanese).
5. Chen F, Zhang X, Ma K, Madajewski B, Benezra M, Zhang L, Phillips E, Turker MZ, Gallazzi F, Penate-Medina O, *et al*: Melanocortin-1 receptor-targeting ultrasmall silica nanoparticles for dual-modality human melanoma imaging. ACS Appl Mater Interfaces 10: 4379-4393, 2018.
6. Guo W, Wang H, Yang Y, Guo S, Zhang W, Liu Y, Yi X, Ma J, Zhao T, Liu L, *et al*: Down-regulated miR-23a contributes to the metastasis of cutaneous melanoma by promoting autophagy. Theranostics 7: 2231-2249, 2017.
7. Ye Z, Dong H, Li Y, Ma T, Huang H, Leong HS, Eckel-Passow J, Kocher JA, Liang H and Wang L: Prevalent homozygous deletions of type I interferon and defensin genes in human cancers associate with immunotherapy resistance. Clin Cancer Res 24: 3299-3308, 2018.
8. Chen X, Chen P, Chen SS, Ma T, Shi G, Zhou Y, Li J and Sheng L: *miR-106b-5p* promotes cell cycle progression of malignant melanoma by targeting *PTEN*. Oncol Rep 39: 331-337, 2018.
9. Jiang L, Tu Y, Hu X, Bao A, Chen H, Ma X, Doyle T, Shi H and Cheng Z: Pilot study of ^{64}Cu(I) for PET imaging of melanoma. Sci Rep 7: 2574, 2017.
10. Yu J, Wu X, Yan J, Yu H, Xu L, Chi Z, Sheng X, Si L, Cui C, Dai J, *et al*: Anti-GD2/4-1BB chimeric antigen receptor T cell therapy for the treatment of Chinese melanoma patients. J Hematol Oncol 11: 1, 2018.
11. Sonoda Y, Kijima M and Uchida H: Melanoma of the choroid. Nihon Ganka Kiyo 19: 828-831, 1968 (In Japanese).
12. Liu SM, Lin CH, Lu J, Lin IY, Tsai MS, Chen MH and Ma N: miR-596 modulates melanoma growth by regulating cell survival and death. J Invest Dermatol 138: 911-921, 2018.
13. Ma Y, Cheng X, Wang F, Pan J, Liu J, Chen H, Wang Y and Cai L: ING4 inhibits proliferation and induces apoptosis in human melanoma A375 cells via the Fas/Caspase-8 apoptosis pathway. Dermatology 232: 265-272, 2016.
14. Lin S, Lv J, Peng P, Cai C, Deng J, Deng H, Li X and Tang X: Bufadienolides induce p53-mediated apoptosis in esophageal squamous cell carcinoma cells *in vitro* and *in vivo*. Oncol Lett 15: 1566-1572, 2018.
15. Raymond-Hamet: Toxicity of orally administered bufotalin. C R Seances Soc Biol Fil 152: 571-574, 1958 (In French).
16. Pettit GR and Kamano Y: Bufadienolides. 21. Synthesis of cinobufagin from bufotalin. J Org Chem 37: 4040-4044, 1972.
17. Zhang DM, Liu JS, Tang MK, Yiu A, Cao HH, Jiang L, Chan JY, Tian HY, Fung KP and Ye WC: Bufotalin from Venenum bufonis inhibits growth of multidrug resistant HepG2 cells through G_2/M cell cycle arrest and apoptosis. Eur J Pharmacol 692: 19-28, 2012.
18. Wen L, Liu L, Wen L, Yu T and Wei F: Artesunate promotes G2/M cell cycle arrest in MCF7 breast cancer cells through ATM activation. Breast Cancer 25: 681-686, 2018.
19. Yin PH, Liu X, Qiu YY, Cai JF, Qin JM, Zhu HR and Li Q: Antitumor activity and apoptosis-regulation mechanisms of bufalin in various cancers: New hope for cancer patients. Asian Pac J Cancer Prev 13: 5339-5343, 2012.
20. Malumbres M and Barbacid M: Cell cycle, CDKs and cancer: A changing paradigm. Nat Rev Cancer 9: 153-166, 2009.
21. Ren Y, Zhang SW, Xie ZH, Xu XM, Chen LL, Lou ZG, Weng GB and Yao XP: Cantharidin induces G_2/M arrest and triggers apoptosis in renal cell carcinoma. Mol Med Rep 14: 5614-5618, 2016.
22. Yang CC, Hung CF and Chen BH: Preparation of coffee oil-algae oil-based nanoemulsions and the study of their inhibition effect on UVA-induced skin damage in mice and melanoma cell growth. Int J Nanomedicine 12: 6559-6580, 2017.
23. Wang C, Liang C, Feng W, Xia X, Chen F, Qiao E, Zhang X, Chen D, Ling Z and Yang H: *ICT1* knockdown inhibits breast cancer cell growth via induction of cell cycle arrest and apoptosis. Int J Mol Med 39: 1037-1045, 2017.

24. Huang WW, Tsai SC, Peng SF, Lin MW, Chiang JH, Chiu YJ, Fushiya S, Tseng MT and Yang JS: Kaempferol induces autophagy through AMPK and AKT signaling molecules and causes G_2/M arrest via downregulation of CDK1/cyclin B in SK-HEP-1 human hepatic cancer cells. Int J Oncol 42: 2069-2077, 2013.
25. Li P, Ding N, Zhang W and Chen L: COPS2 antagonizes OCT4 to accelerate the G2/M transition of mouse embryonic stem cells. Stem Cell Reports 11: 317-324, 2018.
26. Anger M, Stein P and Schultz RM: CDC6 requirement for spindle formation during maturation of mouse oocytes. Biol Reprod 72: 188-194, 2005.
27. Li S and Guo L: Pseudolaric acid B induces G2/M arrest and inhibits invasion and migration in HepG2 hepatoma cells. Xi Bao Yu Fen Zi Mian Yi Xue Za Zhi 34: 59-64, 2018 (In Chinese).
28. She H and Mao Z: Study of ATM phosphorylation by Cdk5 in neuronal cells. Methods Mol Biol 1599: 363-374, 2017.
29. Blackford AN and Jackson SP: ATM, ATR, and DNA-PK: The trinity at the heart of the DNA damage response. Mol Cell 66: 801-817, 2017.
30. Ashley AK and Kemp CJ: DNA-PK, ATM, and ATR: PIKKing on p53. Cell Cycle 17: 275-276, 2018.
31. Hennessy BT, Smith DL, Ram PT, Lu Y and Mills GB: Exploiting the PI3K/AKT pathway for cancer drug discovery. Nat Rev Drug Discov 4: 988-1004, 2005.
32. Xu QG, Yu J, Guo XG, Hou GJ, Yuan SX, Yang Y, Yang Y, Liu H, Pan ZY, Yang F, *et al*: IL-17A promotes the invasion-metastasis cascade via the AKT pathway in hepatocellular carcinoma. Mol Oncol 12: 936-952, 2018.